Plasma-Related Atomic Physics with an Electron Beam Ion Trap

Nobuyuki NAKAMURA

Institute for Laser Science, The University of Electro-Communications, Tokyo 182-8585, Japan

(Received 20 May 2013 / Accepted 12 July 2013)

This paper reviews plasma-related atomic physics experiments performed with an electron beam ion trap (EBIT). In particular, activities with two types of EBITs at the University of Electro-Communications are reported after introducing the principle and the design of the devices. Spectroscopic and collisional data which are useful for plasma diagnostics, technology development based on plasmas are presented.

Keywords: electron beam ion trap, highly charged ion, atomic spectrum

DOI: 10.1585/pfr.8.1101152

1. Introduction

An electron beam ion trap (EBIT) [1] is a powerful device to obtain the atomic data of highly charged ions needed for understanding and controlling high temperature plasmas, such as fusion plasmas and the solar corona. It can trap highly charged ions interacting with a monoenergetic electron beam for many hours. It is thus regarded as a well-defined simple plasma consisting of unidirectional monoenergetic electrons and trapped ions with a narrow charge state distribution. Consequently the EBIT plasma is an unique and ideal source for high resolution spectroscopic studies of highly charged ions. Spectra from an EBIT are useful to survey and identify previously unreported lines, and also to provide benchmark for plasma models. An EBIT can also be used as a device to study the interactions of electrons with highly charged ions. Such spectroscopic and collisional data can be obtained for ions over wide ranges of charge state and atomic number; any ion of any element can practically be studied. Interaction energy between ions and electrons can also be varied over a wide range, such as ~ 100 eV to more than 100 keV.

In this paper, we review plasma-related atomic physics experiments performed with two types of EBITs at the University of Electro-Communications; one is a high-energy EBIT called the Tokyo-EBIT [2–4] and another is a low-energy, compact EBIT called CoBIT [5]. The operational principle of an EBIT and the design of the two EBITs are also briefly introduced.

2. Electron Beam Ion Trap (EBIT)

An EBIT [1] was developed at the Lawrence Livermore National Laboratory based on the principle of an electron beam ion source (EBIS) [6] developed at Joint Institute for Nuclear Research in Dubna. Figure 1 shows the schematic principle of an EBIT. An EBIT consists of a Penning-like ion trap and a high-energy, high-density electron beam going through the trap. Its main components are an electron gun, a drift tube (ion trap), an electron collector, and a superconducting magnet. The drift tube is composed of three (or more) successive cylindrical electrodes where a well potential is applied for trapping ions axially. Radial ion trap is achieved by the combination of the strong axial magnetic field produced by the magnet and the space charge potential of the high density electron beam compressed by the magnetic field. Highly charged ions are produced by successive electron impact ionization of the trapped ions. Emission of highly charged ions excited by the electron beam can be studied spectroscopically through a slit opened at the middle of the drift tube. Since the trapped ions are produced and excited by an (quasi-) monoenergetic electron beam, an EBIT has following advantages over plasma sources. (1) A narrow charge state

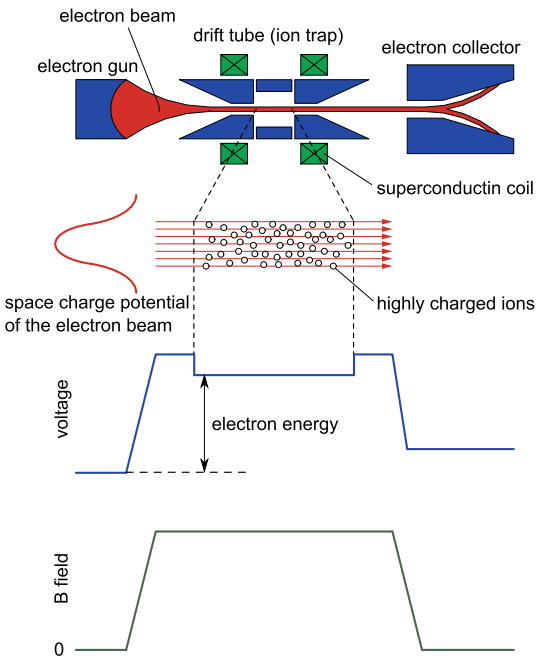

Fig. 1 Schematic principle of an electron beam ion trap.

author's e-mail: n_nakamu@ils.uec.ac.jp

Table 1 Comparison between the Tokyo-EBIT and CoBIT at the University of Electro-Communications.

	Tokyo-EBIT	CoBIT
max. electron energy (keV)	180	2.5
max. electron current (mA)	330	20
max. B-filed (T)	4.5	0.2
cryostat temperature (K)	< 4.2	77
coolant	LHe	LN_2
height (m)	~ 4	~ 0.4

distribution can be obtained with a dominant charge state controlled by the electron energy. (2) Electron energy dependent emission processes, such as resonant excitation, can be studied. (3) There is no Doppler shift and less Doppler broadening. (4) Polarization of radiation excited by a unidirectional electron beam can be studied.

An element of interest is usually introduced through the slit on the drift tube as a molecular beam. Not only rare gases and molecular gases, compounds which have a relatively high vapor pressure can also be used. For example, for producing iron and tungsten ions, ferrocene ($Fe(C_5H_5)_2$) and tungsten hexacarbonyl ($W(CO)_6$) are used respectively.

We have developed a high-energy EBIT called the Tokyo-EBIT [2–4] in 1995 and a compact low-energy EBIT called CoBIT [5] in 2007. The parameters of the two EBITs are listed in Table 1. The details of the two EBITs are described in the following subsections.

2.1 High energy EBIT: Tokyo-EBIT

Figure 2 shows the whole view of the Tokyo EBIT. The electron gun part was designed to be floated at −300 kV. The electron beam emitted from the gun is accelerated toward the drift tube which is designed to be floated at +40 kV at the maximum. Radiation from the ions trapped at the drift tube can be observed at observation ports through eight slits opened radially at the drift tube. The electron collector is designed to be floated at the same voltage as the electron gun, e.g. −300 kV, to absorb the electron beam with a maximum current of 300 mA after decelerating it. The electronic and magnetic fields have been carefully designed to have a laminar flow electron beam traveling from the gun to the collector without hitting any electrodes. Thus a 300 mA power supply is not needed for applying −300 kV to the gun and the collector. Actually the current capacity of the −300 kV power supply is only 1 mA, which enables a ripple as small as < 10 Vrms. Although the maximum electron energy is designed to be 340 keV from the potential difference between the cathode (−300 kV) and the drift tube (+40 kV), the achieved maximum energy so far is 180 keV. Even so, very highly charged ions such as H-like Bi^{82+} and bare Ba^{56+} have been successfully produced. To produce such very highly

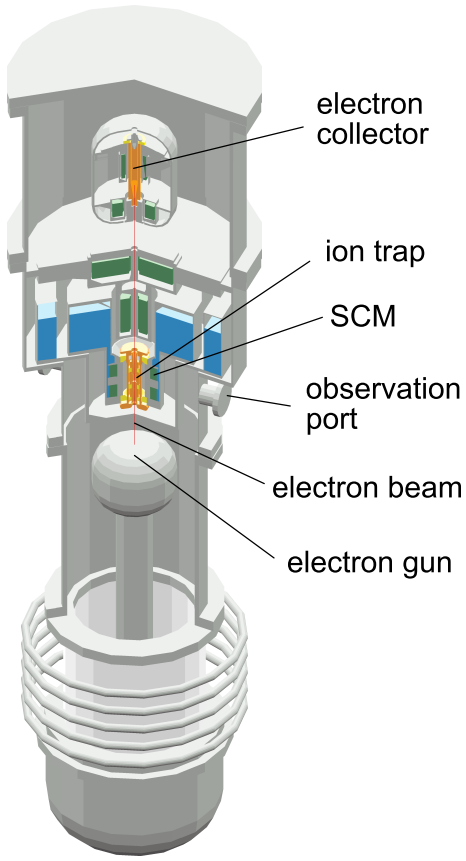

Fig. 2 Schematic of the Tokyo-EBIT. "SCM" represents the superconducting magnet.

charged ions, which have a quite large charge exchange cross section, it is primarily important to obtain an extreme high vacuum condition inside the drift tube. The cryostat for the superconducting magnet acts as a cryopump to keep the vacuum inside the drift tube at <~ 10^{-10} Pa.

2.2 Compact EBIT: CoBIT

Since an EBIT was originally developed for studying few-electron heavy ions to test fundamental quantum theories, almost all EBITs in the world have been designed to be operated with rather high electron beam energy (~ 10 keV or more). With such a high-energy electron beam, light and moderate elements are easily ionized to few-electron or bare ions. On the other hand, for most practical plasmas, atomic data of moderate charge state ions which still keep many electrons are important. For example, to develop an EUV light source for the next-generation lithography, the atomic data of highly charged Sn and Xe ions with charge states around 10 are strongly needed [7, 8]. Another example is the diagnostics of astrophysical and fusion plasmas. For example, the atomic data of highly charged iron ions with charge states around 10 are needed for the spectroscopic diagnostics of the solar corona with observatory satellites [9]. For the next-generation fusion device ITER, the spectroscopic data of

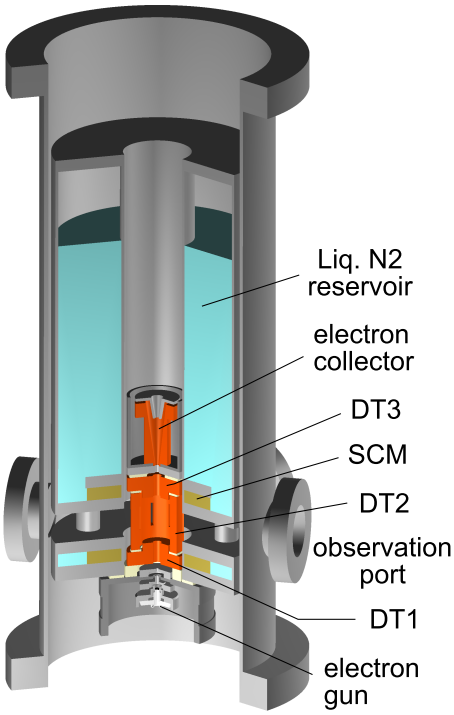

Fig. 3 Schematic of the compact electron beam ion trap CoBIT. "DT" represents the drift tube.

tungsten ions with moderate charge states (~ 20) are needed [10]. To efficiently produce such moderate charge state ions with an EBIT, it should be operated with an electron energy of several hundreds of eV. Although several EBITs have often been operated with such a low energy electron beam, it has more or less difficulties because they have not been designed for such operation.

Thus we have developed a low-energy compact EBIT for the operation with an electron energy of 1 keV or low. Figure 3 shows the schematic view of the compact EBIT, called CoBIT. Restriction of electron energy and current enabled the substantial reduction of the device size as shown in Table 1. The running cost has also been greatly reduced by employing a superconducting wire with a high critical temperature for the central magnet. CoBIT has been originally developed at the University of Electro-Communications under the collaboration with National Astronomical Observatory of Japan and National Institute for Fusion Science (NIFS) to obtain the atomic data of iron ions used for the diagnostics of the solar corona. More recently, a clone [11] has been produced and installed at NIFS to accumulate the atomic data useful for atomic processes in plasmas systematically.

2.3 Apparatus for observation

A typical spectrometer arrangement for CoBIT is shown in Fig. 4. For the spectroscopic studies in the visible range, a commercial Czerny-Turner spectrometer is used. A biconvex lens is placed at the observation port to focus the emission at the entrance slit of the spectrometer.

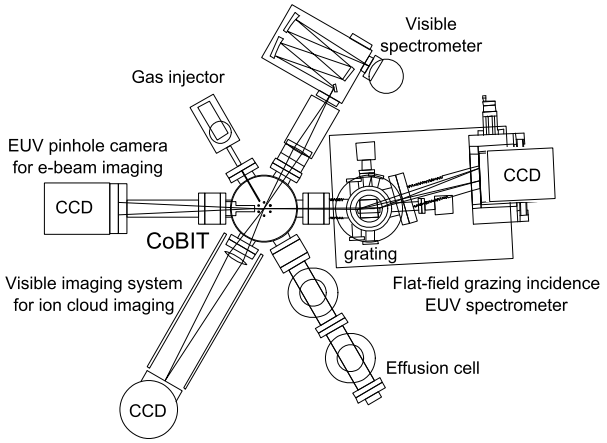

Fig. 4 Diagnostic apparatus for observation with CoBIT.

The diffracted light is detected by a liquid nitrogen cooled CCD. A similar setup is also used for the observation with the Tokyo-EBIT although the size and the focal length of the lens are different.

For the spectroscopic studies in the extreme ultraviolet (EUV) to soft x-ray range, we built grazing incidence flat-field spectrometers [12, 13]. Since an EBIT is a thin line-shaped source, the gratings can be used in a slit-less configuration. Unlike the visible range, highly efficient mirrors and lenses are not available for the wavelength range shorter than VUV, the slit-less configuration has much advantage for efficient observation. A Peltier-cooled CCD is used to detect the diffracted light at the focal plane. Since there is no standard reference source for the EUV range, wavelength calibration for EUV spectra is usually done by emission lines of trapped highly charged ions whose emission wavelength is previously known.

In order to study the density dependent behavior of spectra, a pinhole-camera-like device is attached to CoBIT. A slit 0.2 mm wide is placed at 30 mm from the electron beam and the EUV photons passing through the slit are observed with a back-illuminated CCD placed at 320 mm from the slit. This arrangement enables us to obtain the spatial distribution of the EUV emission with a magnification of about 10. The EUV emission distribution is considered to represent the electron density distribution since the lifetime of EUV transitions is as short as the order of 10^{-10} s. On the other hand, the spatial distribution of the visible emission is also measured using a simple imaging system consisting of a biconvex lens and a liquid-nitrogen cooled CCD. Since most of visible transitions in highly charged ions are magnetic dipole (M1) transitions between fine structure levels, the lifetime is usually as long as the order of 10^{-3} s, which is long enough compared to the motion of the trapped ions. Thus the spatial distribution of the visible emission is considered to represent the spatial distribution of ions, which is needed to determine the overlap factor between the electron beam and the trapped ion

cloud.

For the hard x-ray spectroscopy with the Tokyo-EBIT, a high-resolution Bragg crystal spectrometer [14] is used. The Bragg spectrometer is also used in the slit-less configuration even for flat and von Hámos configurations, which generally require an entrance slit.

3. Survey and Identification of Previously Unreported Lines

Tungsten is considered to be the main impurity in the ITER plasma, and thus spectroscopic data of tungsten ions are necessary to diagnose and control the high temperature plasma in ITER [15]. In particular, there is strong demand for emission lines in the visible range in the diagnostics of the edge plasmas [16]. Since efficient optical components, such as mirrors, lenses, optical fibers, etc., are available, efficient and effective diagnostics can be expected with the visible range. Until recently, however, only one visible emission line [17] has been reported for tungsten ions with a charge state higher than two. Survey and identification of previously unreported visible lines of tungsten ions are thus in strong demand. An EBIT is a suitable device for such a purpose. As an example, tungsten spectra obtained with CoBIT are shown in Fig. 5. As seen in the figure, observed lines revealed strong dependence on electron energy, i.e., they appeared at a certain threshold energy and their intensity became weak when the energy was further increased. This strong dependence reflects the charge distribution in the trap. For example, after the electron energy was changed from 630 eV to 675 eV, production of W^{23+} became available because the ionization energy of W^{22+} is 643 eV [18]. The lines at around 409 and 432 nm, appeared at 675 eV, are thus considered to be emission lines from W^{23+}. When the energy was further increased to 725 eV, which is higher than the ionization energy of W^{23+} (690 eV), the intensity of these lines became small because the number of W^{23+} was decreased due to further ionization, and the line from W^{24+} appeared at around 419 nm.

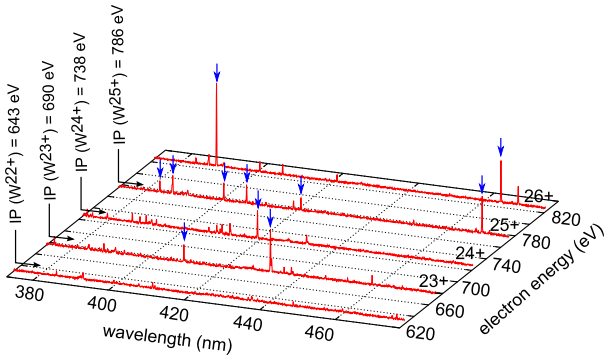

Fig. 5 Visible spectra of highly charged tungsten ions observed with CoBIT. "IP(W^{q+})" represents the ionization potential of W^{q+}.

The validity of such identification based on the appearance energy has been confirmed through several previous experiments [5, 19, 20]. Consequently, the lines indicated by arrows in the figure are assigned to be the transition of tungsten ions shown in each spectrum. Since transitions between different electronic configurations in highly charged heavy ions should fall in shorter wavelength range, such as EUV and x-ray, transitions in the visible range can be assigned as M1 transitions between fine structure levels. The detailed identification of the fine structure levels should be done through comparison with theoretical calculations. Although it is rather difficult to calculate fine structure splitting precisely for many electron heavy ions, some lines in Fig. 5 have been identified through the comparison with detail calculations [19, 21]. Survey of previously unreported lines is also possible with plasma sources, but observation of spectra excited by a mono-energetic electron beam in an EBIT is quite useful for the identification of the responsible charge state as shown here.

4. Transition Lifetime Measurements

Magnetic dipole transitions in the visible range shown in the previous section generally have a transition lifetime in the order of ms. Transition lifetime in such a range can be measured with an EBIT by observing the decay of the transition intensity after turning off the electron beam. Even without an electron beam which produces a space charge trapping potential, ions can still be trapped only with the axial magnetic field and the axial well potential. Figure 6 shows an example of the transition lifetime mea-

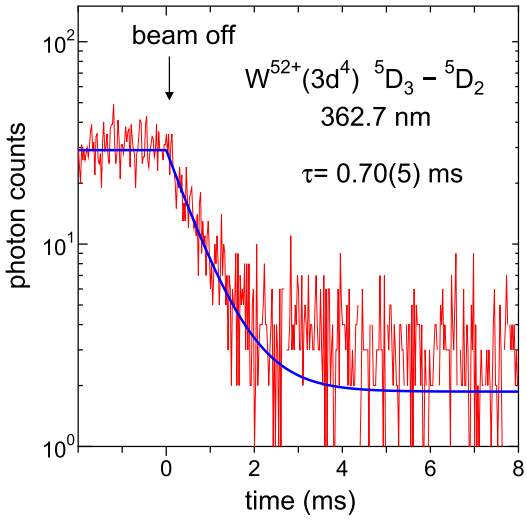

Fig. 6 Time (t) dependence of the intensity of the magnetic dipole transition W^{52+} ($3d^3_{3/2}3d_{5/2}$ $^5D_3$ - $^5D_2$ at 362 nm observed with the Tokyo-EBIT (preliminary result). At t = 0, the electron beam was turned off. By fitting an exponential function to the decay curve after the beam was turned off, the transition lifetime (τ) is estimated to be 0.70 (5) ms.

surement performed for the magnetic dipole transition between fine structure levels of the ground state in Ti-like W^{52+} ($3d^3_{3/2}3d_{5/2}$ $^5D_3$ - $^5D_2$, 362 nm) [17]. In this measurement, the transition was observed with a photomultiplier tube through an interference filter, which has a transmission band width enough narrow to exclude any other transitions. By fitting an exponential function to the experimental decay curve after the electron beam was turned off, a transition lifetime of 0.70(5) ms was obtained. According to theoretical calculation [22], the transition lifetime of the $^5D_3$ - $^5D_2$ transition is estimated to be 4.1 ms. However, the upper level $^5D_3$ can also decay to the $^5D_4$ level[1]. Including the contribution from the transition to $^5D_4$, the transition lifetime is theoretically estimated to be 0.71 ms, which agrees with the experimental value.

5. Polarization and Angular Distribution of Radiation

Polarization and angular distribution are important for diagnostics of nonthermal component in plasmas [23]. For example, in solar flares, the presence of magnetic fields creates nonthermal directional electrons, so that the radiation from such flares can be polarized and have anisotropic distribution [24]. In an EBIT, trapped ions are excited by an electron beam; it is thus useful to observe polarization of radiation excited by an unidirectional electrons.

As an example, Fig. 7 shows the polarization of the Lyman-α_1 ($2p_{3/2} \rightarrow 1s$) transition in hydrogenlike Ti measured with the Tokyo-EBIT [25]. In this measurement, the Lyman-α_1 and α_2 ($2p_{1/2} \rightarrow 1s$) transitions were observed with a high resolution Bragg crystal spectrometer [14] at 90° with respect to the electron beam. Since the total angular momentum of the upper level is 1/2, the Lyman-α_2 transition is intrinsically unpolarized and has an isotropic distribution as far as an unpolarized electron beam is used for excitation. On the other hand, since the total angular momentum of the upper level is 3/2, Lyman-α_1 can have non-zero polarization and anisotropic distribution, reflecting magnetic sublevel distribution in the upper level. When Lyman-α_1 have anisotropic distribution, its intensity ratio to Lyman-α_2 at 90° has a value different from the statistical weighted ratio (2 in this case). In other words, it is possible to obtain the angular distribution (and also the polarization) of Lyman-α_1 from its intensity ratio to Lyman-α_2 at 90°. As seen in the figure, significant discrepancy between the experimental and theoretical values was found. This experiment has been followed by other groups for Ar and Fe, and the discrepancy with theory has also been confirmed. Recently, the discrepancy was explained by the contribution of the Breit interaction [27], which was neglected in the previous theory plotted in Fig. 7.

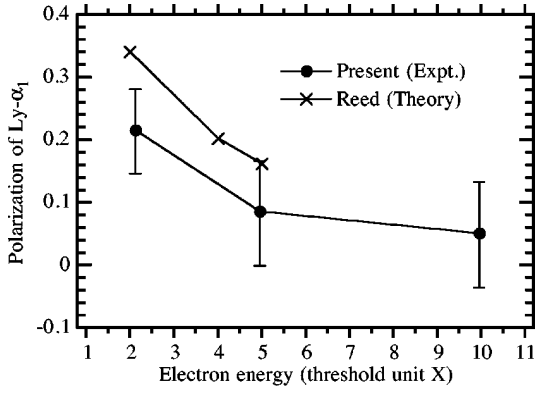

Fig. 7 Polarization of the Lyman-α_1 transition in hydrogenlike Ti as a function of electron energy. Closed circles represent experimental values, and crosses represent theoretical values obtained by the distorted-wave method [26].

[1]For highly charged heavy ions, the order of fine structure levels can be different from that determined by the Hunt's rule. For the ground state ^5D_J ($J = 0 - 4$) of Ti-like W, the order is $J = 0, 1, 4, 2, 3$ in ascending order of energy.

Recently, the angular distribution has also been measured for x-rays emitted in dielectronic recombination (DR) of heavy ions [28]. DR is a combination of dielectronic resonant capture (the inverse process of Auger decay) of an incident electron by an ion and radiative decay of doubly excited states created by the dielectronic resonant capture. When unidirectional beam electrons are used as incident electrons, the magnetic sublevel distribution of the intermediate doubly excited state has unequal distribution in general. The x-ray emitted from the intermediate state has thus anisotropic angular distribution. In the dielectronic resonant capture, the Breit interaction should be taken into account in the interaction between the incident electron and the electron in the target ion. However, the contribution of the Breit interaction is generally small even for heavy ions so that it can be considered as a small correction with respect to the main term, i.e. the Coulomb interaction. In contradiction to this general understanding, recently we found anomalous large contribution of the Breit interaction, that dominates the angular distribution of the X-ray emission in DR of Li-like heavy ions [28].

6. Benchmark Data for Electron-Density Dependent Atomic Models

The plasma in an EBIT is a simple non-neutral plasma composed of trapped ions and quasi-monoenergetic beam electrons. Emission spectra obtained with an EBIT can thus provide a high quality benchmark for testing model calculations used for plasma diagnostics. For example, spectra of iron ions obtained with CoBIT has been used to test the density-dependent model used in the solar corona diagnostics [29]. The electron density of an EBIT is in the order of 10^9 to 10^{12} cm^{-3}, which overlaps with that in the solar corona; an EBIT is thus useful to simulate the solar corona circumstance experimentally in a laboratory. Figure 8 shows typical EUV spectra of highly charged iron

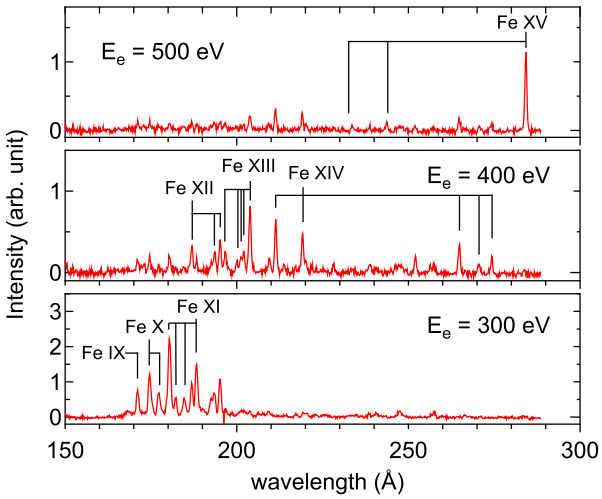

Fig. 8 Typical spectra obtained with CoBIT. E_e denotes the electron beam energy at which the spectrum was obtained.

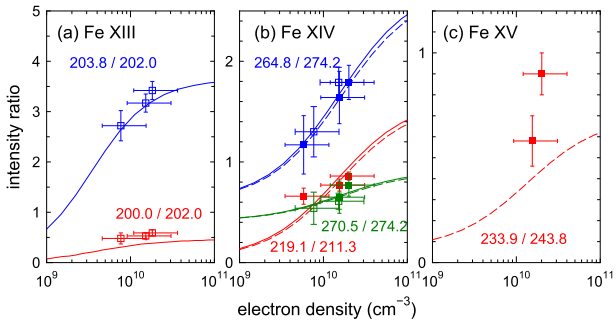

Fig. 9 Intensity ratio of density-sensitive lines of (a) Fe XIII, (b) Fe XIV, and (c) Fe XV. See text for the details.

ions obtained with CoBIT at electron energies of 300, 400, and 500 eV. The spectra indicate that the plasma in CoBIT had a narrow charge state distribution with only two or three predominant charge states. This narrow charge distribution is important for obtaining clean spectra with less line-overlap. Some transitions in Fig. 8 have a fine structure excited state in the ground state electron configuration as a lower level. Such a fine structure excited level decays to a lower fine structure level via M1 transition; electron impact excitation from a fine structure excited level is thus unlikely at the low electron density limit. However, excitation from a fine structure excited level becomes possible as electron density increases; thus, the intensity of the transition to a fine structure excited state increases. The intensity ratio of such a line to a density-insensitive line is used for the electron density diagnostics of the solar corona. We have measured the electron-density dependence of such line ratios. The electron density of the electron beam was changed by changing electron current or central magnetic field or both. The density of the beam electrons was determined from the current and the beam radius measured with the x-ray pinhole device shown in Fig. 4.

The results are shown in Fig. 9. The data obtained with electron beam energies of 400 and 500 eV are plotted as open and closed squares, respectively. The solid and long dashed lines represent the results of the model calculation [29, 30] for 400 and 500 eV, respectively. The numbers in the figure represent the wavelength of the line of interest (e.g., "203.8/202.0" represents the intensity ratio between the lines at 203.8 Å and 202.0 Å). The vertical error bars (1σ) were estimated from fitting with the Gaussian peak profiles. The horizontal error bars have different meanings depending on its sign. The positive error bar represents the maximum electron density at the center of the Gaussian electron beam assumed. The negative error bar represents the effect of the overlap between the electron beam and the trapped ion cloud [29]. As seen in the figure, agreement between the model and the experiment is generally good. However, there seems to be some difference for the 233.9/243.8 ratio of Fe XV. We consider that improvements of the model calculation is needed to explain the experimental result. Theoretical analysis with inclusion of resonant excitation is ongoing as well as the detailed experimental studies on electron energy dependence.

7. Disentangling Plasma Spectra

Emission from plasmas has attracted much attention as a light source in several field. For example, Sn or Xe plasma is expected as a 13.5 nm light source for the next generation EUV lithography [31]. Furthermore, for beyond EUV lithography, emission at around 6.7 nm from Gd and Tb plasmas are investigated recently [32]. Another example is Bi plasmas, which is expected for a light source for the water window region [33]. For the efficient development of such light sources, reliable theoretical models are needed to optimize the emission efficiency at the target wavelength. To test the theoretical model, magnetically confined plasmas are often used [34]. However, since the plasma spectra contain contributions from many charge states, it is rather difficult to understand the spectral features in detail. An EBIT is useful to disentangle the complicated spectrum of plasmas containing contributions from many charge states.

For example, Fig. 10 (a) shows the EUV spectrum of Xe obtained with the Compact Helical System (CHS) plasma [34]. Strong band-like emission due to unresolved transition array (UTA) [35] is found around 11 nm. In addition, sharp lines are found, including prominent lines at around 16.5 nm and 17.5 nm. On the other hand, the EUV spectra (intensity map) of xenon obtained with CoBIT are shown in Fig. 10 (b) [20]. The spectra were obtained by increasing electron energy from 200 to 1000 eV step by step with an interval of 10 eV. The UTA emission around 11 nm is found for energies between 250 and 650 eV. Judging from the energy dependence, xenon ions with charge

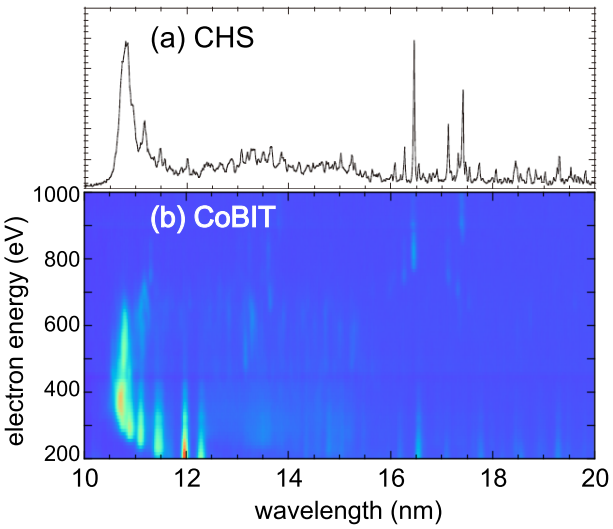

Fig. 10 (a) Xe spectra observed with Compact Helical System (CHS) at NIFS [34]. (b) Xe spectra observed with CoBIT with electron energies of 200 to 1000 eV.

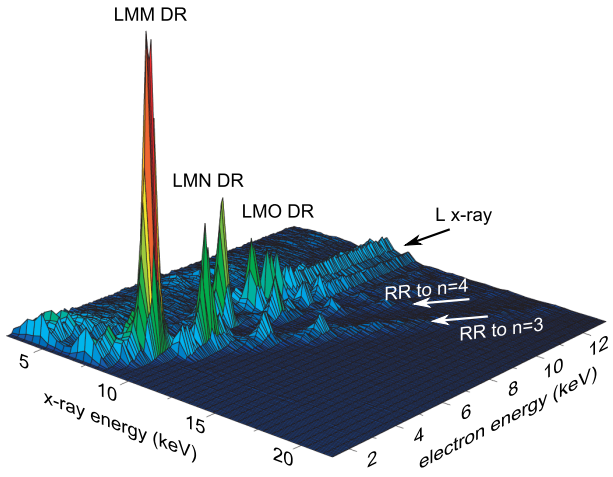

Fig. 11 X-ray spectra of highly charged tungsten ions observed with the Tokyo-EBIT while scanning electron energy between 1.5 an 14 keV. "DR" represents dielectronic recombination. See text for the detail.

states of 11–22 are considered to be responsible for the UTA emission, which is consistent with previous observations [35, 36]. In addition, the line emissions at 16.5 nm and 17.5 nm can be identified as transitions in Xe^{24+} and Xe^{25+}, respectively [20].

8. Collisional Cross Sections

Collisions of highly charged ions with electrons are the most important atomic process in hot plasmas. Various parameters and behavior of plasmas are modeled based on the cross sections for electron collisions, such as excitation, ionization, recombination, etc. For the most simple example, the ion density ratio at the ionization equilibrium is determined from the ratio between ionization and recombination rates. However, even for this simple example, different theories sometimes give quite different results [37]. It is thus obviously important to measure cross sections experimentally and examine the theories with them.

In an EBIT, a quasi-monoenergetic electron beam interacts with trapped highly charged ions. Collision processes, such as excitation [38] and ionization [39, 40] can thus be studied by observing emission from an EBIT or charge state distribution in an EBIT. In particular, resonant processes, such as dielectronic recombination (DR) can be studied efficiently by observing the dependence on electron energy. For example, Fig. 11 shows the x-ray spectra of tungsten ions observed with a Ge detector while scanning electron energy between 1.5 keV an 14 keV. As seen in the figure, x-ray intensity is prominently enhanced due to DR at some electron energies. For example, at an electron energy of ~ 3 keV, L x-rays are enhanced by the LMM DR resonance. LMM represents the process where a doubly excited state is produced by capturing the incident electron into the M shell while exciting a L shell electron to the M shell. For heavy ions, since the doubly excited state decays by emitting x-ray with a probability near unity, x-ray intensity is enhanced at the resonant energy. On the other hand, x-rays whose energy increases with the gradient of unity as a function of electron energy are due to non-resonant recombination (radiative recombination: RR). DR resonant strengths can be obtained by normalizing the x-ray intensity from DR to that from RR, for which reliable cross section can be calculated because there is no need to include electron correlation. For example, so far such a method was used to obtain DR resonant strengths for H-like Kr [41], He-like Ti [42], etc.

9. Summary

As shown in this paper, an EBIT is an unique and versatile device for studying spectra and collision processes of highly charged ions. Three EBITs (the Tokyo-EBIT and two CoBIT) in Japan and over ten EBITs in the world are currently in operation for accumulating the atomic data of highly charged ions relevant to hot plasmas. Spectroscopic data of tungsten ions over a wide range of charge states have been accumulated under the IAEA Coordinated Research Projects "Spectroscopic and Collisional Data for Tungsten from 1 eV to 20 keV" for making a contribution to the future diagnostics of the ITER plasma. Spectra of iron obtained with a well-defined EBIT plasma are used to examine the electron-density dependent plasma model used in solar corona diagnostics. EBIT spectra excited by a monoenergetic electron beam contain contributions from only a few charge states, thus can be used to disentangle complex plasma spectra containing contributions from a wide range of charge states. The disentanglement is needed to understand the laser produced plasma spectra of

Sn, Xe, Gd, Tb, Bi, etc., which are expected as short wavelength light sources. An EBIT is a powerful device also for studying collisional processes of highly charged ions, and the monoenergeticity of the electron beam enables ones to study resonant processes, such as dielectronic recombination which strongly affects the ionization balance and the emission of plasmas.

Acknowledgments

This work was performed with the support and under the auspices of the NIFS Collaboration Research program (NIFS09KOAJ003) and JSPS KAKENHI Grant Number 23246165, and partly supported by the JSPS-NRF-NSFC A3 Foresight Program in the field of Plasma Physics (NSFC: No.11261140328).

[1] R.E. Marrs *et al.*, Phys. Rev. Lett. **60**, 1715 (1988).
[2] N. Nakamura *et al.*, Phys. Scr. **T73**, 362 (1997).
[3] F.J. Currell *et al.*, J. Phys. Soc. Jpn. **65**, 3186 (1996).
[4] H. Watanabe *et al.*, J. Phys. Soc. Jpn. **66**, 3795 (1997).
[5] N. Nakamura *et al.*, Rev. Sci. Instrum. **79**, 063104 (2008).
[6] E.D. Donets and V.P. Ovsyanniko, Sov. Phys. JETP **53**, 466 (1981).
[7] G. O'Sullivan *et al.*, AIP Conf. Proc. **771**, 108 (2005).
[8] H. Ohashi *et al.*, J. Phys.: Conf. Ser. **58**, 235 (2007).
[9] T. Watanabe *et al.*, AIP Conf. Proc. **901**, 215 (2007).
[10] R. Radtke *et al.*, J. Phys.: Conf. Ser. **58**, 113 (2007).
[11] H.A. Sakaue *et al.*, JINST **5**, C08010 (2010).
[12] H.A. Sakaue *et al.*, J. Phys.: Conf. Ser. **163**, 012020 (2009).
[13] H. Ohashi *et al.*, Rev. Sci. Instrum. **82**, 083103 (2011).
[14] N. Nakamura, Rev. Sci. Instrum. **71**, 4065 (2000).
[15] N.J. Peacock *et al.*, Can. J. Phys. **86**, 277 (2008).
[16] C.H. Skinner, Can. J. Phys. **86**, 285 (2008).
[17] H. Watanabe *et al.*, Phys. Rev. A **63**, 042513 (2001).
[18] A.E. Kramida and T. Shirai, At. Data Nucl. Data Tables **95**, 305 (2009).
[19] A. Komatsu *et al.*, Phys. Scr. **T144**, 014012 (2011).
[20] J. Yatsurugi *et al.*, Phys. Scr. **T144**, 014031 (2011).
[21] X.-B. Ding *et al.*, J. Phys. B **44**, 145004 (2011).
[22] D. Kato *et al.*, J. Chin. Chem. Soc. **48**, 525 (2001).
[23] T. Fujimoto and S.A. Kazantsev, Plasma Phys. Control. Fusion **39**, 1267 (1997).
[24] J.M. Laming, Astrophys. J. **357**, 275 (1990).
[25] N. Nakamura *et al.*, Phys. Rev. A **63**, 024501 (2001).
[26] K.J. Reed and M.H. Chen, Phys. Rev. A **48**, 3644 (1993).
[27] C.J. Bostock, D.V. Fursa and I. Bray, Can. J. Phys. **89**, 503 (2011).
[28] Z. Hu *et al.*, Phys. Rev. Lett. **108**, 073002 (2012).
[29] N. Nakamura *et al.*, Astrophys. J. **739**, 17 (2011).
[30] N. Yamamoto *et al.*, Astrophys. J. **689**, 646 (2008).
[31] G. O'Sullivan *et al.*, J. Phys.: Conf. Ser. **163**, 012003 (2009).
[32] S.S. Churilov *et al.*, Physica Scripta **66**, 293 (2002).
[33] B. Li *et al.*, Appl. Phys. Lett. **102**, 041117 (2013).
[34] C. Suzuki *et al.*, J. Plasma Fusion Res. **81**, 480 (2005).
[35] H. Tanuma *et al.*, J. Phys.: Conf. Ser. **58**, 231 (2007).
[36] C. Biedermann *et al.*, Nucl. Instrum. Methods B **235**, 126 (2005).
[37] T. Nakano and The JT-60 Team, J. Nucl. Mater. **415**, S327 (2011).
[38] N. Nakamura *et al.*, J. Phys. Soc. Jpn. **69**, 3228 (2000).
[39] B. O'Rourke *et al.*, J. Phys. B **34**, 4003 (2001).
[40] H. Watanabe *et al.*, Nucl. Instrum. Methods B **205**, 417 (2003).
[41] Z. Hu, Y. Li and N. Nakamura, Phys. Rev. A **87**, 052706 (2013).
[42] B. O'Rourke *et al.*, J. Phys. B **37**, 2343 (2004).